

Task-driven SLAM Benchmarking

Yanwei Du¹, Shiyu Feng², Carlton G. Cort¹, Patricio A. Vela¹

Abstract—For assistive robots, one critical use case of SLAM is to support localization as they navigate through an environment completing tasks. Current SLAM benchmarks do not consider task-based deployments where repeatability (precision) is more critical than accuracy. To address this gap, we propose a task-driven benchmarking framework for evaluating SLAM methods. The framework accounts for SLAM’s mapping capabilities, employs precision as a key metric, and has low resource requirements to implement. Testing of state-of-the-art SLAM methods in both simulated and real-world scenarios provides insights into the performance properties of modern SLAM solutions. In particular, it shows that passive stereo SLAM operates at a level of precision comparable to LiDAR-based SLAM in typical indoor environments. The benchmarking approach offers a more relevant and accurate assessment of SLAM performance in task-driven applications.

Keywords: SLAM, navigation, closed-loop, precision.

I. INTRODUCTION

Service robots have increasingly been deployed into home and work environments, and other parts of daily life [1]–[7]. Their primary goal is to provide repeatable services and possibly interact with human workers, in the process enhancing productivity and fostering more efficient work environments. Central to the operation of these mobile robots is SLAM, whose localization capabilities support navigation. A robust and reliable SLAM system is pivotal for completing of tasks that are distributed throughout a given environment. Despite recent advancements in SLAM achieving high accuracy in existing benchmarks and datasets [8]–[11], service robots using SLAM continue to face challenges with robustness. They lose track of their location within the map, which leads to task failure and requires human intervention to restore service [12]. These failures are not adequately addressed by existing benchmarks, which typically evaluate SLAM methods based on trajectory accuracy using metrics such as Absolute Trajectory Error (APE) or Relative Pose Error (RPE). Focus on APE/RPE has led many SLAM methods to prioritize improving accuracy metrics, while not addressing whether they actually translate to improved task-oriented autonomy. For service robots using SLAM, the main concern is whether the robot can reliably navigate to the same location when needed. Precise knowledge of its absolute position is not necessary for performing subsequent tasks, as these rely on other perception-based modules to follow through on the

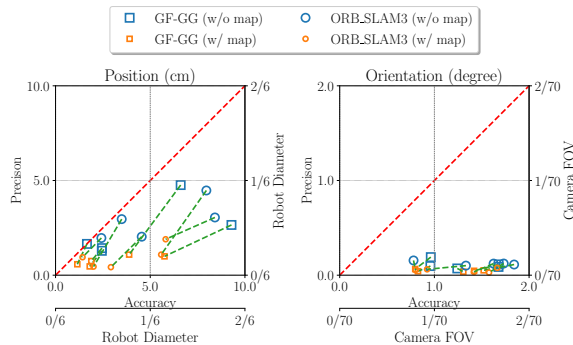


Fig. 1: Visual SLAM performance in the EuRoC Machine Hall sequences. Each marker represents a sequence for a given method, with its size and color indicating whether the SLAM map was used. The plots demonstrate that precision more effectively reflects SLAM performance from a task-driven perspective and that incorporating a SLAM map improves overall performance. Please refer to the experiment section §III-C for details.

service activity at the given goal location. In such task-driven scenarios, the robot only needs sufficient localization success to transition between tasks. What matters most is robust, repeatable performance to ensure successful task execution. Repeatability is best measured using precision.

While significant efforts have recently been devoted to rich, multi-sensor fusion capable benchmarking [9], [13], the performance gap between SLAM benchmarking via open-loop, sensor stream replay versus task-oriented performance has motivated other to evaluate SLAM and related autonomy modules through different lenses. Simulated worlds figure prominently due to reproducibility of outcomes, ease of implementation by researchers, and the availability of ground truth information. Embodied AI research, such as the Habitat Navigation Challenge [14], exemplifies the necessity for a task-driven evaluation methodology. The simulation-based challenge emphasizes the need for robust, long-term navigation capabilities. The potential of localization to support autonomous vehicles has also led to the design of a simulation-based benchmarking scheme for street navigation [15] with success/failure as the main metric. While deployed during runtime, the localization module is not in the decision loop and thereby neglects the module’s full impact on system performance. SLAM latency plays a role in its robustness and accuracy, with some relationship found between these two factors for the task of trajectory tracking using SLAM pose estimates as feedback [16], [17]. The simulation-based benchmarking in [16], [17] demonstrate the need to move beyond just accuracy when considering SLAM in the closed-loop. A reasonable next step would be to more explicitly consider navigation.

Real-world benchmarking remains mostly open-loop due

*Supported in part by NSF Awards #1816138, 2235944, & 2345057.

¹Y. Du, C. G. Cort, and P. A. Vela are with the School of Electrical and Computer Engineering, and Institute of Robotics and Intelligent Machines, Georgia Institute of Technology, Atlanta, GA 30308, USA. {yanwei.du, ccort6, pvela}@gatech.edu

²S. Feng is with the School of Mechanical Engineering and the School of Electrical and Computer Engineering, Georgia Institute of Technology, Atlanta, GA 30308, USA. shiyufeng@gatech.edu

to the need for accuracy to have absolute, global ground truth signals for comparison. Significant effort is required to obtain such ground truth sources. For instance, KITTI [8] depends on RTK-GPS for highly precise vehicle positioning, while HILTI [9] employs a total station (a high precision laser scanner), both of which are costly. Datasets like EuRoC [10] and the TUM family [18] use motion-capture systems, which are difficult to implement in large-scale indoor, multi-room environments. Similarly, methods like PennCOSYVIO [19] rely on fiducial markers, introducing artificial features that can bias the evaluation of SLAM systems. Other methods [13], [20] rely on LiDAR-SLAM or multi-sensor fusion results as ground truth. However, these approaches do not accurately reflect the real-time performance of SLAM when integrated with other modules that are interconnected and mutually influential. The Subterranean (SubT) Challenge [21] is a real-world evaluation that tests the closed-loop system (e.g., one integrating SLAM and navigation) where robots explore underground environments and localize targets distributed throughout it. However, in addition to target detection, it prioritizes accuracy of target locations as performance assessment focuses on absolute position accuracy in a global frame. The evaluation criteria is more about giving the true location of the target rather than being able to reliably guide a human back to the target. Resource intensive surveying methods were used to generate the ground truth. It’s methodological design mirrors that of [22], whose indoor evaluation approach combined ceiling-mounted visual markers with total station surveying. Our objective is to reduce the need for high accuracy, costly absolute measurement technology or reliance on other offline SLAM-type methods for ground truth.

An additional difference between these benchmarks and the deployment of service robots is that the latter often incorporate an initial mapping stage prior to being tasked. Existing benchmarks overlook this phase by evaluating performance solely through one-time data playback. SLAM maps are pivotal as they mitigate long-term drift and ensure consistency (high precision) across multiple visits to the same locations [23], [24]. Multi-session SLAM evaluation [25] does consider map reuse with accuracy and precision performance metrics for repeated runs to the same locations. However, the study design and variables may consider different performance factors and experimental methodology for LiDAR SLAM [25], and also for visual SLAM multi-map and map reuse open-loop tests [23], [24]. These works point to the need for reproducible and standardized benchmarking schemes for SLAM systems equipped with pre-built maps. Further evidence for this need is given in Fig. 1, where the EuRoC dataset is used in a multi-run manner (see §III-C for more details). The precision vs accuracy plots show better precision than accuracy indicating that SLAM evaluation may under-report performance. Including a mapping phase further improves performance, especially position precision. Referencing the performance metrics to robot characteristics (under x -axis) permits qualitative assessment of potential goal attainment success by relating precision to what task

region the robot may see at its arrival pose.

This paper introduces a SLAM benchmark framework with navigation-in-loop that emphasizes task-relevant metrics such as repeatability (precision) and completion. It applies to LiDAR and visual sensor based SLAM approaches and includes a map building phase. The benchmarking approach mimics real-world implementations where robots are typically given ample time to create a complete map for improved task execution during deployment. Through experiments on several visual and LiDAR SLAM methods, we identify which methods effectively support navigation tasks. The key contributions are as follows:

- A low-cost, easy to setup, task-driven SLAM benchmark with precision as the key metric for measuring robot consistency in reaching the same pose over multiple rounds. The method scales to large environments.
- Evaluation of state-of-the-art visual and LiDAR SLAM systems in both simulation and real-world scenarios, with evidence that passive visual methods match the robustness and precision of LiDAR-based methods for indoor settings.
- Open-sourced benchmarking framework to benefit the broader SLAM research community [26].

II. METHODOLOGY

A. Preliminaries

The following symbols and definitions are used:

- **Robot Pose** - (x, y, θ) - robot’s current position and orientation in the environment. SLAM pose estimates in $SE(3)$ are projected to $SE(2)$.
- **Sequence** - \mathbf{S} - A set of waypoints the robot is required to sequentially follow, i.e., $\mathbf{S} = \{\mathbf{w}_1, \mathbf{w}_2, \dots, \mathbf{w}_N\}$.
- **Waypoint** - $\mathbf{w}_i = (x_i, y_i, \theta_i)$ indexed by i - position and orientation (heading angle) of the robot in the 2D plane.
- **Indexing** - Index i represents the waypoint index, and j represents the round index, k as the sequence index.
- **Counts** - N denotes the number of waypoints in a sequence, and M is the number of rounds in a test, K is sequence count.

A variable with a * symbol denotes its ground truth or reference value, and a $\bar{}$ symbol denotes mean value.

B. Real-World Benchmarking Framework

Mobile robot task execution requires collision-free navigation to designated target locations, in addition to SLAM localization. Centered on this objective, our benchmark framework incorporates navigation as part of the evaluation implementation and uses SLAM for closed-loop operation. Fig. 2 depicts the navigation framework as implemented in ROS [27]. The chosen navigation scheme uses the TEB local planner [28].

1) *Task Definition:* Waypoint Navigation. We define waypoints representing typical navigation tasks, as exemplified in the Amazon Gazebo hospital model [29] shown in Fig. 3. These waypoints are manually specified based on a floorplan-like map in the environment’s free space. The robot starts from a fixed location and sequentially navigates to

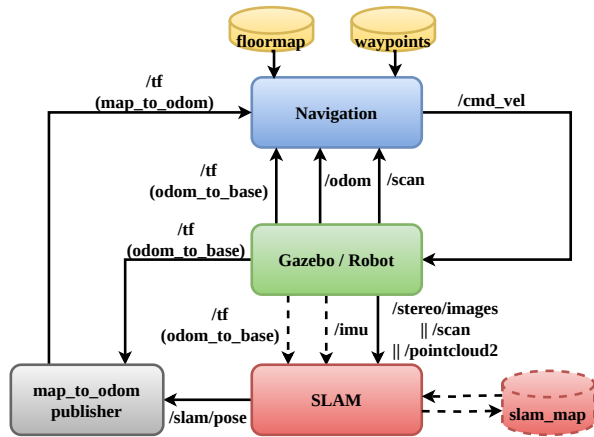


Fig. 2: Navigation framework. The dashed arrows and cylinder are optional elements, utilized depending on the specific SLAM methods and testing configurations. The symbol || represents alternatives, which also depend on the SLAM methods.

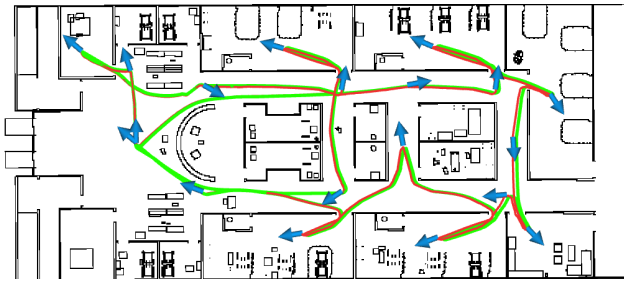


Fig. 3: The definition of waypoints (marked as blue arrows) in the AWS Gazebo hospital world, with the robot estimated (red) and ground truth trajectories (green) plotted when executing the navigation task.

each waypoint. Upon reaching a waypoint, the robot's pose is recorded for evaluation. The procedure is repeated for multiple rounds, terminating if the robot fails to reach any waypoint. It is assumed that the map accurately reflects the environment, with no dynamic obstacles or unknown areas.

2) *Performance Metrics*: Accuracy, Completeness, and Precision. Typically, accuracy metrics such as Absolute Trajectory Error (ATE) or Relative Pose Error (RPE) are used to evaluate open-loop SLAM performance [18]. Navigation and trajectory tracking evaluation of SLAM employ task-specific metrics [15], [16]. Here performance evaluation of indoor mobile robot navigation will emphasize waypoint navigation reliability and repeatability, measured by successful goal attainment percentage (completeness) and goal pose precision. Accuracy, in the form of APE, will apply only for the simulated scenarios, where such ground-truth is available.

Let $\mathbf{z} = (x, y)$ represent the robot location. The accuracy of navigation to waypoint \mathbf{w}_i captures how close the robot gets to the target goal over multiple rounds. It involves computing the average position and orientation errors,

$$e_{\mathbf{w}_i} = \frac{1}{M} \sum_j^M \|\mathbf{z}_{ij} - \mathbf{z}_i^*\|_2 \quad \text{and} \quad \delta_{\mathbf{w}_i} = \frac{1}{M} \sum_j^M \|\theta_{ij} - \theta_i^*\| \quad (1)$$

where the orientation error factors for wrap-around.

The precision of a waypoint \mathbf{w}_i quantifies the proximity of robot pose measurements to each other over multiple rounds,

again decomposed into position and orientation,

$$E_{\mathbf{w}_i} = \frac{1}{M} \sum_j^M \|\mathbf{z}_{ij} - \bar{\mathbf{z}}_i\|_2 \quad \text{and} \quad \Delta_{\mathbf{w}_i} = \frac{1}{M} \sum_j^M \|\theta_{ij} - \bar{\theta}_i\| \quad (2)$$

where means are computed over all rounds (index j).

Completeness (C) refers to the ratio of completed waypoints over all waypoints of all sequences:

$$C = \frac{\sum_{k=1}^K \sum_{i=1}^{N_k} \delta_{ki}}{\sum_{k=1}^K N_k} \quad \text{for} \quad \delta_{ki} = \begin{cases} 0, & \text{if } M_{ki} < M \\ 1, & \text{otherwise} \end{cases} \quad (3)$$

where N_k is the waypoint count in sequence S_k , and M_{ki} is the successful waypoint \mathbf{w}_i attainment count for the M runs.

3) Real-World Completeness and Precision Measurement:

Instead of focusing on high accuracy in an absolute coordinate system, our benchmark prioritizes waypoint precision, which assesses the repeatability of the robot's navigation across multiple rounds relative to its own internal coordinate system, as inferred from an external static reference frame.

To measure this in real-world conditions, we use an overhead camera system (Fig. 4) mounted on the ceiling to track the robot's pose at each waypoint; each camera requires connection to a computer or laptop. An AprilTag is affixed to the top of the robot for pose estimation from the camera system (Fig. 4). AprilTag detection validation [30] indicates that tag detection point error is within 0.5 pixel for the AprilTag C++ library, making it suitable for evaluation purposes. Waypoint attainment success is established by the AprilTag being fully visible to the camera, otherwise the robot failed to reach the waypoint's vicinity. Any downward facing camera would do, including one temporarily installed on a tripod, or otherwise statically placed, facing the ground region the robot is specified to navigate to. Waypoint precision does not rely on absolute references. It is assessed independent of other waypoints and the evaluation is possible in local coordinate systems defined by the cameras observing them. Multiple cameras deployed for different waypoints do not require global calibration nor mutual awareness. Each camera/waypoint measurement pair operates independently.

This method offers two significant advantages: 1) The camera setup is straightforward and easy to install at the necessary measurement points. It does not require global calibration, specialized expertise, nor expensive specialized equipment for operation, as is required in a motion capture system or a surveying strategy. 2) Unlike fiducial markers used in some existing approaches, the overhead camera does not introduce artificial features into the environment that could potentially bias SLAM performance. A tripod setup might, but would be minimal compared to fiducial markers that are designed to be visually distinct.

From a task-driven perspective, as long as the robot can successfully transition to subsequent tasks, accuracy is less critical. High precision is more important as it demonstrates that the SLAM system can consistently complete the navigation task by arriving at the target location in its own coordinate system, which is crucial for practical applications. As the simulation experiments provide accuracy

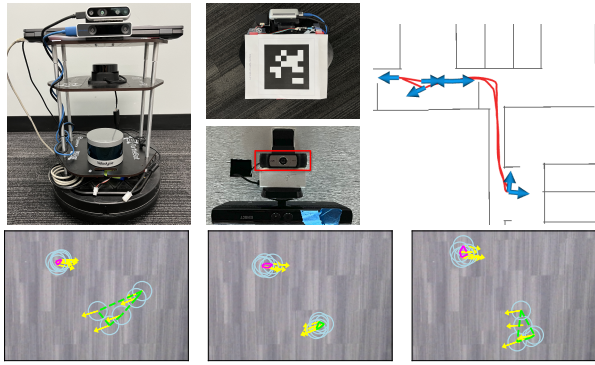


Fig. 4: Real world experimental setup. Clock-wise from top-left: A Turtlebot2 is equipped with the SLAM sensors and laptop, on top of which is placed an AprilTag. Downward facing cameras (in red box) and computers/laptops are placed in the environment to detect and recover the robot’s pose. The robot waypoints, defined to be under the cameras, should be accurate enough that the robot will be visible when reached. During the programmed tour, the cameras will detect and estimate the robot pose when seen. Precision and completeness follows from the estimates.

and precision from available ground truth information, they provide a comprehensive understanding of these two metrics and their correlation.

4) *Map-Based Performance Evaluation*: To demonstrate the impact of map reuse on task completion, we run additional tests for SLAM methods that support mapping. Since some methods cannot save and load maps, we introduce an extra priming round where the robot traverses the waypoints and builds a map online. This map is then used for subsequent rounds without resetting the robot’s pose to the initial location after each round. The robot poses recorded during the mapping phase are excluded from evaluation. Comparing the results from tests with and without the use of a pre-built SLAM map highlights the benefits of a prior SLAM map for task-oriented SLAM performance.

III. EXPERIMENT DESIGN

The effectiveness of the proposed benchmark framework will be established through a series of controlled experiments. Simulation experiments assess SLAM performance using all metrics: accuracy, precision, and completeness. The accuracy and precision metrics are also related to the robot’s diameter and the camera’s field of view (FOV) to quantify position and orientation performance in robot relative terms. Doing so more strongly connects performance variability to the robot and its task. If a robot is too far from an object, relative to its size, or headed in a bad direction, relative to its visual field of view, then a follow-up visually guided approach, manipulation, or object viewing task would fail.

A. SLAM Candidates

For comparative analysis a diverse set of SLAM methods are tested, spanning LiDAR and passive stereo sensors. All methods include inertial and robot odometry signals as required or when permitted. The parameters were not tuned for optimal performance across the tests, with default settings used; they are generally effective in most scenarios and offer balanced performance. Our goal is not to identify the best

TABLE I: Scenario Properties in Simulation and Real-World

| Name | Key Features | Area (m^2) | Path Length (m) |
|-------------|---------------------------------|----------------|---------------------|
| Small House | Home furniture layouts | 144 | 45 |
| Warehouse | Shelves with boxes & goods | 260 | 70 |
| Hospital | Rooms w/medical equipment | 1400 | 220 |
| TSRB Office | Multiple long corridors | 1500 | 260 |
| TSRB Real | A long corridor and sharp turns | 225 | 45 |

SLAM method, but rather to identify suitable methods and to validate the value of our proposed benchmark framework and obtain generally reasonable and reproducible outcomes for study in robot-relative terms.

1) *2D LiDAR*: SLAM-Toolbox [31] and HectorSLAM [32]. They leverage scan matching to correct robot odometry drift and are commonly used for indoor navigation.

2) *Stereo Visual and Visual-Inertial*: GF-GG [17] & ORB_SLAM3 [23], feature-based stereo visual methods; DSOL [33], a direct sparse odometry system; SVO-Pro [34], a semi-direct method; and MSCKF [35], a filter-based method. ORB_SLAM3 would often fail to initialize when using inertial measurements, even with extra movement prior to testing. It is run as stereo-only.

3) *3D LiDAR-Inertial*: FAST-LIO2 [36] and LIO-SAM [37]. They are commonly deployed for autonomous driving, and were used by SubT Challenge competitors [38], [39].

B. Closed-Loop Experiments

The closedloop tests are conducted in both simulated and real-world environments. The scenarios are listed in Table I. In each scenario, the robot starts from a fixed initial location, typically the origin of the map, and navigates sequentially through the waypoints. The planning frequency is kept constant across all experiments to ensure consistency. Upon reaching each waypoint, the robot pauses for 5 seconds before proceeding to the next one. The computer/laptop at this waypoint, which is synchronized with NTP (delay < 1 second), saves timestamped image data upon detecting the tag affixed to the robot. The robot’s poses are estimated offline and associated with waypoints by timestamps for performance evaluation.

A single scenario is tested for five consecutive rounds. In each round, the robot is either reset or continues next round based on the testing modes—without and with a SLAM map. The same resetting strategy applies to the SLAM methods used. For details on the map-based evaluation, please refer to the methodology section §II-B.4. A waypoint is considered successfully completed only if the robot arrives at it in all five rounds; failure to reach a waypoint in any round results in it being marked as incomplete. The accuracy and precision for each completed waypoint (successfully reached in all five rounds) are calculated according to Eq. (1) and (2).

1) *Simulation*: Gazebo [40] is chosen for benchmark test in simulation due to its highly realistic simulated environment. It provides readily available sensor data, including camera and LiDAR feeds and accurate ground truth data, enabling precise evaluation of system performance.

2) *Real World*: Testing was extended to the real world in an office building with the Turtlebot2 robot (Diameter: 37.5cm), see Fig. 4, which offers odometry measurements through its built-in sensors. Additionally, we utilize an RPL-iDAR S2 for 2D LiDAR-based SLAM methods, a Realsense D435i (FOV: 87°) for visual (and visual-inertial) methods, and a Velodyne-16 for 3D LiDAR SLAM methods. We use 30 cm and 80.0° as robot scale constants in the evaluation. The laser data is also integrated into the navigation module for obstacle avoidance. All the processes run on an Intel Core i7-9850 laptop (single-thread passmark score of 2483).

We define a sequence spanning approximately 45 meters, featuring six waypoints (Fig. 4). This includes a stretch through a corridor beginning at waypoint 2, followed by sections that require rapid rotational movements by the robot at waypoint 3. Subsequently, the robot retraces its path through waypoints 4 and 5, returning to its starting location.

Following the real world measuring method described in section §II-B.3, three overhead cameras (Fig. 4) are used to capture these waypoints, each covering two waypoints. If a camera fails to observe the robot at a waypoint, that waypoint is recorded as a failure for that round.

C. Open-loop EuRoC Dataset - A Preliminary Study

As indicated in the introduction, provisional analysis of open-loop SLAM benchmarking indicates that SLAM performance evaluation may benefit from a task-driven perspective. This section describes the benchmarking performed and how it promotes the benchmarking method described in this paper. The machine hall sequences may be viewed as an aerial vehicle performing a search or inspection task, where the objective is to consistently identify and revisit specific points during repeat inspections. Evaluation involves pose estimation accuracy and precision, with each frame treated as an inspection point the robot should reach.

1) *Setup*: Two stereo methods with map-to-frame pose tracking functionality are evaluated: ORB_SLAM3 and GF-GG. For SLAM map reuse, each sequence restarts without resetting the SLAM method to keep the map in memory for subsequent runs. Eq. (1) and (2) are modified for evaluation in $SE(3)$. Based on a review of [10], we estimate the robot’s diameter to lie in the range of 30 to 50 cm, and the camera’s horizontal field of view (FOV) to be 70.8° . The values 30 cm and 70.0° serve as robot scale constants.

2) *Results and Analysis*: The results, visualized in Fig. 1 as precision vs accuracy plots, indicate that position estimation precision is consistently lower than the accuracy across all sequences. Precision is within $1/6$ of a robot diameter without map use. The same holds for orientation, with precision values lower than 0.2 degrees. When utilizing a SLAM map, both methods indicate a performance boost with outcomes shifted toward the lower-left corner. Position precision reduces to $1/12$ of a robot diameter. An object intended to be centered in the field of view from a reasonable distance would still be visible and nearly centered. This suggests that accuracy does not adequately reflect potential

SLAM performance from a task-driven perspective, and points towards the benefits of replacing it with precision.

D. Closed-Loop Benchmarking Outcomes and Analysis

The simulation outcomes will first be analyzed as the accuracy metrics permit correlation and comparison with precision. After, the real-world outcomes will be analyzed. Both point to precision as a meaningful metric to pair with completeness, and point to passive stereo SLAM as being on par with LiDAR-based SLAM.

1) *Simulation*: The Fig. 5a precision vs accuracy plots for position and orientation consistently show better precision than accuracy when the navigation succeeds; larger markers indicate more success. To some degree this indicates that localization failure is catastrophic when it occurs; there doesn’t seem to be a sliding scale. The completeness vs precision plots in Fig. 5b also indicate the same by plateauing rather than exhibiting linear growth to 100% across the precision axis. In the cases studied, either a SLAM method is precise to a robot diameter (or two), or it fails. Orientation accuracy and precision are both well bounded given the field of view. Due to the strong performance of orientation, it will not be reviewed in future analysis.

Of the methods tested, only SLAM-Toolbox and GF-GG achieved perfect performance. ORB_SLAM3’s low performance results from program crashes during runs, an unresolved issue reported in its repository [41]. These crashes are more frequent in long-path, large-scale scenarios, suggesting the system issue arises in long-term navigation tasks. The least complete implementations are odometry methods (DSOL, SVO-Pro), as they cannot leverage map content, nor long baseline associations outside of the filtering window. With similar performance are the 3D-LiDAR methods and MSCKF. The 3D LiDAR methods underperformed, given their strong results in existing benchmarks and near universal preference in robot deployments [21]. This may be due system parameters settings or the piecewise-uniform structure of indoor environments. Hector SLAM got closest to perfect, but exhibits enough failures to not be reliable. None of the methods with failures substantially benefit from map use, in the sense of rising to perfect completeness. The SLAM-Toolbox and GF-GG curves are shifted left, which indicates improved precision (the vertical line at 1 robot diameter in Fig 5b serves as a visual reference for comparison).

Deeper study of SLAM-Toolbox and the stereo methods will consider accuracy and precision, as provided by the violin plots of Fig. 6. Comparing left (blue) to right (orange), map use shifts the tail portion of the distribution to the core region. Comparing accuracy to precision, the precision distributions appear to be compressed versions of the accuracy distributions indicating the potential for a relationship between the two implementations. The results show map use as beneficial to precision, and precision as being well distributed in relation to the robot diameter. While SLAM-Toolbox is more precise, with nearly four times the precision (1.75 cm vs. 6.41 cm), GF-GG task performance should not

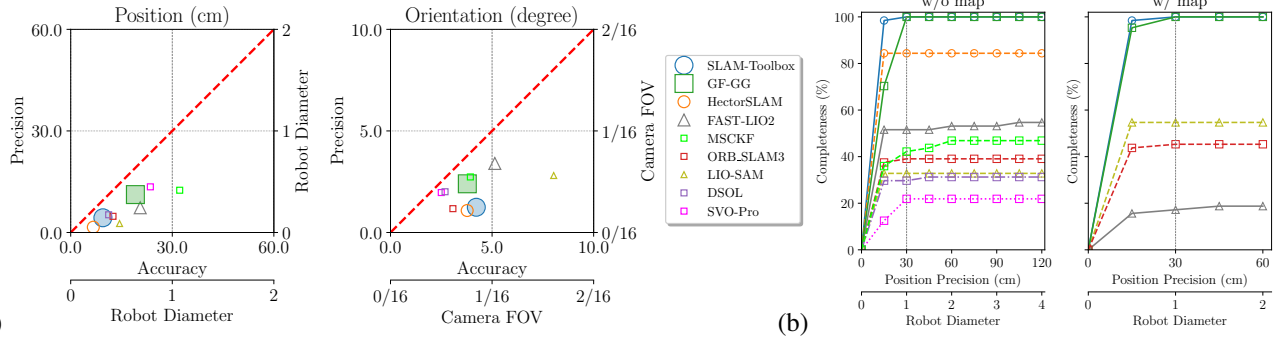


Fig. 5: Waypoint Precision vs. Accuracy in plot (a). Marker size represents waypoint completeness (larger is better), with full completeness methods filled. The red diagonal marks the boundary where precision equals accuracy. Waypoint Position Completeness vs. Precision in plot (b).

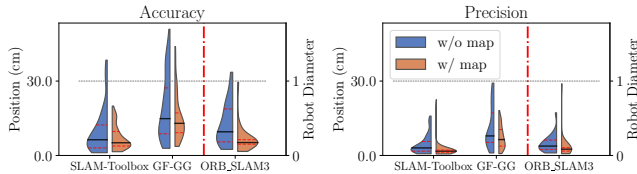


Fig. 6: Waypoint Position Accuracy and Precision distribution w/o and w/ SLAM map. Methods are ordered by completeness, ties are broken by accuracy in the w/ map mode. The vertical dashdotted red bars indicate full completeness boundary.

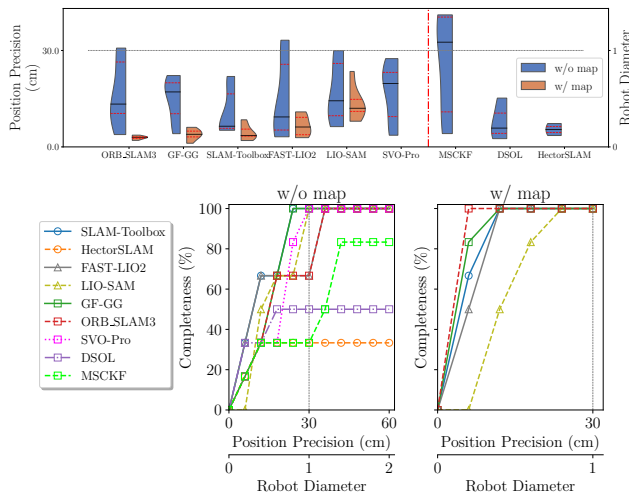


Fig. 7: Top: Waypoint Position Precision distribution in real-world testing. Methods are ordered by completeness in w/ map mode, with precision value as the tiebreaker. Methods without a map are ordered in w/o map mode. Bottom: Waypoint Position Completeness vs. Precision plot.

be impacted by the lower precision. From a task perspective, both are equivalent.

2) *Real-World*: To start, the average orientation precision lies below 10 degrees for all methods, which is $1/8$ of the camera’s field of view. This level of precision is considered acceptable from a task-driven perspective. Analysis will cover only position precision. Fig. 7 provides completeness vs precision results for the real-world tests, without and with map use. Focusing on the w/o map case, Hector-SLAM, DSOL, and MSCKF do not achieve 100% completeness, which mirrors the simulation. In contrast, the LIO approaches and SVO-Pro do. ORB_SLAM3 and FAST-LIO2 are the last to reach 100% completeness just past 1 robot diameter. Before that are SVO-Pro and LIO-SAM at around 1 robot

diameter. The first to reach 100% completeness are SLAM-Toolbox and GF-GG. The improved performance for some of the methods is most likely due to the smaller area and shorter path length (~ 45 m) of these tests relative to simulation. Importantly, passive stereo implementations continue to exhibit comparable performance to LiDAR-based implementations.

Moving to review the plot for the map use case, there is a left-ward shift in the curve indicating improved precision and an overall compression in the variance across methods. ORB_SLAM3 exhibits the best performance, followed by SLAM-Toolbox, GF-GG, and FAST-LIO2. Last to rise is LIO-SAM. Except for LIO-SAM, these methods are precise to within $2/5$ of a robot diameter (ORB_SLAM3 is within $1/5$). *All are acceptable regarding task completion.* In the map use case, the passive stereo implementations are amongst the top performing; the top three in rank order are ORB_SLAM3, GF-GG, and SLAM-Toolbox (2D LiDAR). The stereo sensor implementations more effectively leverage the map, due to map-to-frame matching and loop-closure. Evidence for this lies in the precision violin plots of Fig. 7 and in the average precision of 2.9, 3.9, and 4.5 cm for ORB_SLAM3, GF-GG, and SLAM-Toolbox, respectively. Please see the multimedia attachment for visual evidence from the overhead cameras, to qualitatively see how precision varies across the methods.

IV. CONCLUSION

This work introduces a task-driven SLAM benchmark. Focusing on precision highlights its importance in task-oriented applications where repeatability is essential. The benchmark considers the mapping capabilities of SLAM systems, an aspect often overlooked in existing evaluations. Assessing how effectively a system can utilize maps, provides a more comprehensive understanding of SLAM performance and suitability for real-world tasks. The results demonstrate that visual SLAM methods can achieve precision performance comparable to LiDAR-based methods in indoor navigation tasks. This finding underscores the potential of visual SLAM systems to be reliable and effective alternatives to LiDAR approaches, offering similar levels of precision while potentially reducing costs and increasing accessibility.

REFERENCES

- [1] Z. A. Barakeh, S. Alkork, A. S. Karar, S. Said, and T. Beyrouthy, "Pepper humanoid robot as a service robot: a customer approach," *3rd International Conference on Bio-engineering for Smart Technologies*, pp. 1–4, 2019.
- [2] Amazon Astro. [Online]. Available: <https://www.aboutamazon.com/news/tag/astro>
- [3] B. Tribelhorn and Z. Dodds, "Evaluating the Roomba: A low-cost, ubiquitous platform for robotics research and education," in *IEEE International Conference on Robotics and Automation*, 2007, pp. 1393–1399.
- [4] Moxi. Diligent Robotics. [Online]. Available: <https://www.diligentrobots.com/moxi>
- [5] M. Valdez, M. Cook, and S. Potter, "Humans and robots coping with crisis – starship, covid-19 and urban robotics in an unpredictable world," in *IEEE International Conference on Systems, Man, and Cybernetics (SMC)*, 2021, pp. 2596–2601.
- [6] M. Barten. Hotel Robots: An Overview of Different Robots Used in Hotels. [Online]. Available: <https://www.revfine.com/hotel-robots>
- [7] Knightscope Inc. [Online]. Available: <https://www.knightscope.com>
- [8] A. Geiger, P. Lenz, and R. Urtasun, "Are we ready for autonomous driving? the KITTI vision benchmark suite," in *IEEE Conference on Computer Vision and Pattern Recognition*, 2012, pp. 3354–3361.
- [9] M. Helmberger, K. Morin, B. Berner, N. Kumar, G. Cioffi, and D. Scaramuzza, "The hilti slam challenge dataset," *IEEE Robotics and Automation Letters*, vol. 7, no. 3, pp. 7518–7525, 2022.
- [10] M. Burri, J. Nikolic, P. Gohl, J. Schneider, J. Rehder, S. Omari, M. Achtelik, and R. Y. Siegwart, "The EuRoC micro aerial vehicle datasets," *The International Journal of Robotics Research*, vol. 35, pp. 1157 – 1163, 2016.
- [11] T. Schops, T. Sattler, and M. Pollefeys, "Bad slam: Bundle adjusted direct rgb-d slam," in *IEEE/CVF Conference on Computer Vision and Pattern Recognition*, 2019, pp. 134–144.
- [12] L. Young. (2024, January) Companies Brought in Robots. Now They Need Human 'Robot Wranglers'. [Online]. Available: <https://www.warehouseautomation.ca/news/companies-brought-in-robots-now-they-need-human-robot-wranglers>
- [13] P. Kaveti, A. Gupta, D. Giaya, M. Karp, C. Keil, J. Nir, Z. Zhang, and H. Singh, "Challenges of Indoor SLAM: A multi-modal multi-floor dataset for SLAM evaluation," in *IEEE International Conference on Automation Science and Engineering*, 2023, pp. 1–8.
- [14] K. Yadav, J. Krantz, R. Ramrakhya, S. K. Ramakrishnan, J. Yang, A. Wang, J. Turner, A. Gokaslan, V.-P. Berges, R. Mootaghi, O. Maksymets, A. X. Chang, M. Savva, A. Clegg, D. S. Chaplot, and D. Batra. Habitat Challenge 2023. [Online]. Available: <https://aihabitat.org/challenge/2023/>
- [15] L. Suomela, J. Kalliola, A. Dag, H. Edelman, and J.-K. Kämäräinen, "Benchmarking Visual Localization for Autonomous Navigation," in *IEEE/CVF Winter Conference on Applications of Computer Vision*, 2023, pp. 2945–2955.
- [16] Y. Zhao, J. S. Smith, S. H. Karumanchi, and P. A. Vela, "Closed-loop benchmarking of stereo visual-inertial SLAM systems: Understanding the impact of drift and latency on tracking accuracy," in *IEEE International Conference on Robotics and Automation*, 2020, pp. 1105–1112.
- [17] Y. Zhao, J. S. Smith, and P. A. Vela, "Good Graph to Optimize: Cost-Effective, Budget-Aware Bundle Adjustment in Visual SLAM," *ArXiv*, vol. abs/2008.10123, 2020.
- [18] J. Sturm, N. Engelhard, F. Endres, W. Burgard, and D. Cremers, "A benchmark for the evaluation of RGB-D SLAM systems," in *IEEE/RSJ international conference on intelligent robots and systems*, 2012, pp. 573–580.
- [19] B. Pfrommer, N. Sanket, K. Daniilidis, and J. Cleveland, "PennCOSYVIO: A challenging visual inertial odometry benchmark," in *IEEE International Conference on Robotics and Automation*, 2017, pp. 3847–3854.
- [20] P. Wenzel, R. Wang, N. Yang, Q. Cheng, Q. A. Khan, L. von Stumberg, N. Zeller, and D. Cremers, "4Seasons: A Cross-Season Dataset for Multi-Weather SLAM in Autonomous Driving," *Pattern Recognition*, vol. 12544, pp. 404–417, 2020.
- [21] T. H. Chung, V. Orekhov, and A. Maio, "Into the Robotic Depths: Analysis and Insights from the DARPA Subterranean Challenge," *Annual Review of Control, Robotics, and Autonomous Systems*, vol. 6, no. 1, pp. 477–502, 2023.
- [22] H. Kikkeri, G. Parent, M. Jalobeanu, and S. Birchfield, "An inexpensive method for evaluating the localization performance of a mobile robot navigation system," *IEEE International Conference on Robotics and Automation*, pp. 4100–4107, 2014.
- [23] C. Campos, R. Elvira, J. J. G. Rodríguez, J. M. M. Montiel, and J. D. Tardós, "ORB-SLAM3: An Accurate Open-Source Library for Visual, Visual-Inertial, and Multimap SLAM," *IEEE Transactions on Robotics*, vol. 37, no. 6, pp. 1874–1890, 2021.
- [24] R. Mur-Artal and J. D. Tardós, "Visual-Inertial Monocular SLAM With Map Reuse," *IEEE Robotics and Automation Letters*, vol. 2, no. 2, pp. 796–803, 2017.
- [25] E. Pearson and B. Englot, "A Robust and Rapidly Deployable Waypoint Navigation Architecture for Long-Duration Operations in GPS-Denied Environments," in *20th International Conference on Ubiquitous Robots*, 2023, pp. 319–326.
- [26] Task Driven Visual SLAM Benchmarking. [Online]. Available: https://github.com/ivalab/task_driven_visual_slam_benchmark.git
- [27] M. Quigley, K. Conley, B. Gerkey, J. Faust, T. Foote, J. Leibs, R. Wheeler, and A. Y. Ng, "ROS: an open-source robot operating system," in *IEEE International Conference on Robotics and Automation workshop on open source software*, vol. 3, no. 3.2, 2009, p. 5.
- [28] C. Rösmann, W. Feiten, T. Wösch, F. Hoffmann, and T. Bertram, "Efficient trajectory optimization using a sparse model," in *European Conference on Mobile Robots*, 2013, pp. 138–143.
- [29] AWS Gazebo Model. [Online]. Available: <https://github.com/aws-robotics/aws-robomaker-hospital-world.git>
- [30] S. M. Abbas, S. Aslam, K. Berns, and A. Muhammad, "Analysis and improvements in apriltag based state estimation," *Sensors*, vol. 19, no. 24, p. 5480, 2019.
- [31] S. Macenski and I. Jambrecic, "SLAM Toolbox: SLAM for the dynamic world," *Journal of Open Source Software*, vol. 6, no. 61, p. 2783, 2021.
- [32] S. Kohlbrecher, O. Von Stryk, J. Meyer, and U. Klingauf, "A flexible and scalable SLAM system with full 3D motion estimation," in *IEEE international symposium on safety, security, and rescue robotics*, 2011, pp. 155–160.
- [33] C. Qu, S. S. Shivakumar, I. D. Miller, and C. J. Taylor, "DSOL: A Fast Direct Sparse Odometry Scheme," in *IEEE/RSJ International Conference on Intelligent Robots and Systems*, 2022, pp. 10 587–10 594.
- [34] C. Forster, Z. Zhang, M. Gassner, M. Werlberger, and D. Scaramuzza, "SVO: Semidirect visual odometry for monocular and multicamera systems," *IEEE Transactions on Robotics*, vol. 33, no. 2, pp. 249–265, 2016.
- [35] A. I. Mourikis and S. I. Roumeliotis, "A multi-state constraint Kalman filter for vision-aided inertial navigation," in *IEEE International Conference on Robotics and Automation*, 2007, pp. 3565–3572.
- [36] W. Xu, Y. Cai, D. He, J. Lin, and F. Zhang, "FAST-LIO2: Fast Direct LiDAR-Inertial Odometry," *IEEE Transactions on Robotics*, vol. 38, pp. 2053–2073, 2021.
- [37] T. Shan, B. Englot, D. Meyers, W. Wang, C. Ratti, and D. Rus, "LIO-SAM: Tightly-coupled Lidar Inertial Odometry via Smoothing and Mapping," *IEEE/RSJ International Conference on Intelligent Robots and Systems*, pp. 5135–5142, 2020.
- [38] K. Ebadi, L. Bernreiter, H. Biggie, G. Catt, Y. Chang, A. Chatterjee, C. Denniston, S.-P. Deschênes, K. Harlow, S. Khattak, L. Nogueira, M. Palieri, P. Petr'avceck, M. Petrl'ik, A. Reinke, V. Kr'atk'y, S. Zhao, A. akbar Agha-mohammadi, K. Alexis, C. Heckman, K. Khosoussi, N. Kottege, B. Morrell, M. Hutter, F. Pauling, F. Pomerleau, M. Saska, S. A. Scherer, R. Y. Siegwart, J. L. Williams, and L. Carlone, "Present and Future of SLAM in Extreme Underground Environments," *ArXiv*, vol. abs/2208.01787, 2022.
- [39] A. Koval, C. Kanellakis, and G. Nikolakopoulos, "Evaluation of Lidar-based 3D SLAM algorithms in SubT environment," *IFAC-PapersOnLine*, vol. 55, no. 38, pp. 126–131, 2022.
- [40] N. Koenig and A. Howard, "Design and use paradigms for Gazebo, an open-source multi-robot simulator," in *IEEE/RSJ International Conference on Intelligent Robots and Systems*, vol. 3, 2004, pp. 2149–2154.
- [41] ORB-SLAM3 repository. [Online]. Available: https://github.com/uz-slamlab/ORB_SLAM3/issues?q=sophus+nan